KSME Journal, Vol. 9, No. 2, pp. 251~262, 1995

A New Tracking System for Magneto-Optical Disk Drives. Part Ⅱ : Analysis and Servo System

Kyihwan Park*, Soo-Hyun Kim*, Yoon Keun Kwak* and Heui-Seok Kang**

(Received October 24, 1994)

To reduce the average accessing time of a magneto-optical (MO) disk drive, which is a severe drawback of current products, a newly developed moving-magnet type tracking actuator has been designed and tested. The effort of developing a fast positioning actuator is divided into two parts. One is to develope a new driving mechanism having a fast tracking capability and the other is to adopt an advanced control scheme. In this work, the second effort is mainly addressed using a hybrid control and adaptive model-following control.

Key Words : Moving-Magnet Type Tracking Actuator, Hybrid Control, Adaptive Model-Following Control, Average Accessing Time, Switching Point.

1. Introduction

Magneto-optical disk (MO) is a memory device which reads and writes data optically using a magnetic field. Because the MO disk systems are erasable they are being increasingly used as computer external memory device. The MO disk drive has some advantages over the traditional magnetic floppy disk drive, namely, a higher capacity due to a high track density, and less susceptibility to mechanical wear because only the laser beam affects the surface of the magneto-optical disk. On the other hand, it has one significant disadvantage compared to magnetic system, namely, its slow accessing performance which results in a low data transfer rate. The relatively sluggish performance of MO drives derives from a few factors : The reading/writing mechanisms of MO drives need two degrees of actuation, which are tracking and focusing actuations, and they lead to a heavy actuator. Many optical components required for transmitting and receiving a laser beam also make the system heavy. As another factor, a small track pitch causes tracking difficulties. Note that all of the causes of slow accessing are related to the immaturity of magneto-optical recording systems. Lighter heads, improved actuators, and more powerful lasers will facilitate much faster magneto-optical disk systems. Currently the average accessing time, defined as the time to move 1/3 of a full stroke, in magneto-optical (MO) 5.25 inch disk systems is greater than 100 ms. By comparison, in magnetic disk systems, accessing times as low as 20 ms have been produced.

Two separate tracking servo mechanisms traditionally have been used in the tracking operation as a tandem coarse and fine positioner. In the tracking operation, the moving part or tracking actuator which has an objective lens and a focusing actuator is driven radially to the target track. It is first coarsely positioned to the vicinity of the target track with an accuracy of ± 1 μm. Next it is finely positioned by a fine positioner such as a galvano-mirror with an accuracy of ± 0.1 μm. In this tracking operation, most of the accessing time is spent on coarse positioning. Therefore, it is necessary to develop a coarse positioner which is capable of fast positioning and ± 1 μm accuracy. This effort is the thrust of the research reported here. A fine tracking actuator is not developed in

* Department of Mechanical Engineering, KAIST, 373-1, Kusong-dong, Yusong-gu, Taejon 305-701, Korea

** Department of Mechanical Engineering, The Univ. of Texas at Austin, Texas

this work.

The effort of developing a fast positioning coarse positioner includes two fields: development of a new driving mechanism of fast tracking capability and application of advanced control. As a new driving mechanism, a moving-magnet type actuator was introduced in the previous work (Park, 1994). It has been adopted because it offers a simple and compact design which produces high acceleration. This type of actuator is much less sensitive to temperature changes than the moving-coil type of actuator, and this advantage can serve to improve accuracy. Since only design of the tracking actuator was introduced in the previous work, the speed performance of this driving mechanism should be tested. In this paper, it will be tested by using just conventional control. As another effort of developing fast positioning tracking actuator, an advanced control also can be considered. For this, adaptive model following control is introduced and its merit is demonstrated.

Tracking accuracy is also as important to be improved in MO disk drive as the tracking speed. A disturbance observer is implemented with a state observer to increase an accuracy and its effectiveness is verified by experiment.

This work is composed as follows: in Section 2, design of the tracking actuator which was introduced is briefly described. Servo control system and experimental results in terms of speed and accuracy are provided in Section 3. An advanced control method is discussed in Section 4. In Section 5, this work is concluded and the future work is summarized.

2. Design of the Tracking Actuator

Figure 1 shows the configuration of the developed linear tracking actuator. Four permanent magnets are used above and below the air-core solenoid to have four times as much force as when only one magnet is used. This arrangement cancels unfavorable forces and torques, thus reducing the friction between the bearings and the rod which magnets are attached to. The four magnets are driven simultaneously by the same current.

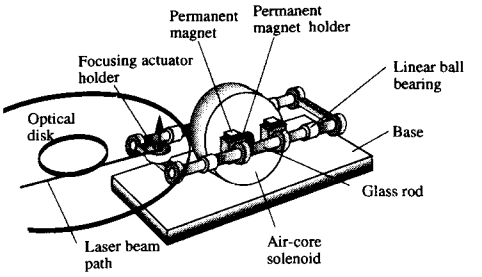

Fig. 1 Configuration of the developed coarse tracking actuator.

Neodymium iron boron (NdFeB) rare-earth magnets are used for magnetic materials because it provides a high remanence with high coercivity.

This moving-magnet type actuator has advantages over the moving-coil type of actuator. First, the moving-magnet type actuator permits a compact (low mass) design of magneto-optical disk systems, which means higher acceleration for the same force.

Second, heat is generated by the coils in either actuator type, but it is easier for the moving-magnet type actuator to dissipate heat because the coils are stationary. Moreover, since the coils are part of the moving structure in a moving-coil actuator, the accuracy might degrade due to temperature changes.

Third, the moving-magnet actuator requires no power source in its moving parts. Thus it can move freely while the moving-coil actuator requires the moving parts to be tethered to a power source.

Fourth, in the moving-magnet type actuator the cost of manufacturing is lower because the permanent magnets can be much smaller than the ones which are used in the moving-coil type actuator. The cost of permanent magnets scales roughly with their volume, and they represent a significant fraction of the material costs in magnetic systems.

To determine the optimal dimension of the air core solenoid and permanent magnets for generating the maximum actuating force, a magnetic circuit theory was used as a tool for developing a simplified mathematical model. Further information regarding this subject can be found in Part I (Park, 1994). With the optimal dimension, the

Table 1 The specifcations of the tracking actuator.

Description	Value
Width of permanent magnet	6 *mm*
Length of permanent magnet	12 *mm*
Height of permanent magnet	4 *mm*
Inner radius of solenoid	2 *mm*
Outer radius of solenoid	28 *mm*(57 turns)
Length of solenoid	15 *mm*(30 layers)
Air gap	1 *mm*
Coil resistance	22.5 Ω
Number of turns	1710
Mass of tracking actuator	0.025 *kg*
Damping coefficient	0.95 *Ns/m*
Force constant	1.6*N/A*

proposed tracking actuator is capable of exerting a force of 1.6 N for a current of 1 A, and the force constant K_t, which is defined as a ratio of the force per unit current, is $1.6N/A$. The force constant will be used as a system gain in control of the tracking system. The specification of the tracking actuator is listed in Table 1.

3. Servo Control System Using a Conventional Controller

3.1 System analysis

The mechanical motion of the proposed tracking actuator can be represented by a second order differential equation in displacement:

$$M\ddot{x} + c\dot{x} = F, \tag{1}$$

$$F = K_t I, \tag{2}$$

where M is a tracking actuator mass and c is a viscous damping coefficient. F is the applied magnetic force to the tracking actuator, K_t is the force constant, and I is the input current. K_t is obtained using a scale and it is 1.6 N/A. M is composed of the permanent magnets, the connecting parts, focusing actuator holder, and the glass rod. It can be easily measured by using a scale and it is about 0.025 *kg*. c is experimentally measured by using the logarithmic decrement method (Park, 1993) and it is estimated 0.95 $N \cdot s/m$.

Using a current amplifier which supplies a current I proportional to its input voltage u, the electric circuit equation can also be expressed by the following equation:

$$I = K_a u, \tag{3}$$

where K_a is a gain of the current amplifier and it is adjusted as 0.2 A/V. The function of the current amplifier is to provide a load current which is independent of the load impedance but strictly proportional to the input voltage. To check its function as an ideal current source, the current amplifier is verified by a frequency response test, and its bandwidth is proved to be around 5 *kHz*. A OP-51 power operational amplifier from Apex is chosen for the current amplifier. Using Eqs. (1) to (2), the block diagram of system dynamics is represented in Fig. 2. v and x are the velocity and position of the tracking actuator.

To position in minimum time with high position accuracy, a bang-bang, velocity, and position controller are incorporated. The advantage of each control mode can be combined to establish the desired performance by switching the system from one control mode to another. In this strategy, the bang-bang control loop is cut off a few tracks ahead of the target track and then the velocity control loop is connected to the velocity command input signal. This permits the tracking actuator to slide smoothly toward the target track by using a velocity trajectory to cover the remaining distance. The velocity trajectory with respect to the remaining distance is calculated from the state equations which will be described in the next subsection. Further, system uncertainties can be compensated with this feedback system. A closed loop controller for the final stage of the decelerating range continuously adjusts the decelerating drive signal to provide the desired accuracy. The velocity trajectory is stored in a look-up table in

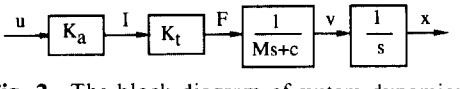

Fig. 2 The block diagram of system dynamics.

advance because it takes time to calculate the velocity trajectories in a real time control process. When the velocity reaches almost zero, the velocity control loop is cut off and the position control loop is connected to the position command input signal. This allows the tracking actuator to settle down onto the target track with the required accuracy. *A P* controller and *PD* controller are used for velocity and position control and are implemented with analog circuits. The control program is implemented by a digital computer. The maximum acceleration and deceleration, switching points, velocity trajectories for the transition range, and the target point are predetermined and stored in the computer.

Actually, the position and velocity information are embedded in the optical disk for tracking to enable an optical head to approach a target track quickly and accurately. Since position information, for example, is written on the disk, no external position sensing system is required. Note that the optical components such as a laser beam and optical pick up devices are required so that the position and velocity information can be directly measured by using an optical disk. With the consideration of cost and scope of the work, we exclude the use of the optical disk as a measurement device, so it is necessary to develop an external measurement device to replace the role of the optical disk. A lateral effect position sensitive device (PSD) is used for replacing the role of the optical disk. The velocity information is obtained by using a state observer which is discussed in the next subsection.

3.2 State observer

The system dynamics can be expressed by the following state space form

$$\dot{x}_1 = x_2, \tag{4}$$

$$\dot{x}_2 = -\frac{c}{M}x_2 + \frac{K_a K_t}{M}u, \tag{5}$$

where x_1, x_2, and u denote the position, velocity,

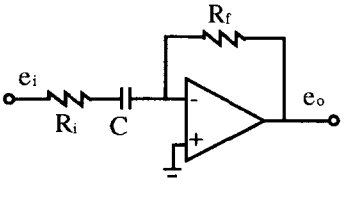

$$\frac{e_o}{e_i} = \frac{R_f C(j\omega)}{1+R_i C(j\omega)}$$

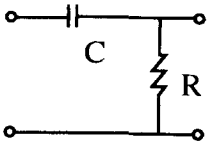

$$\frac{e_o}{e_i} = \frac{j\omega}{RC+j\omega}$$

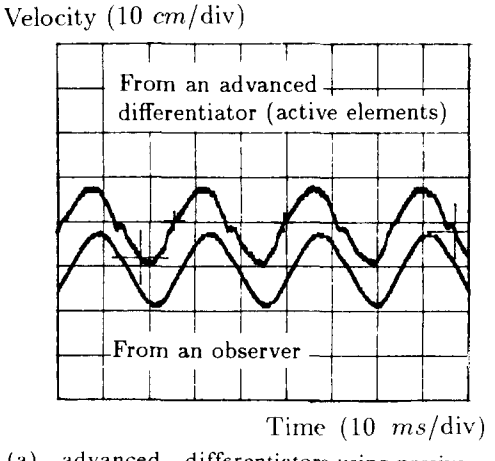

(a) advanced differentiators using passive elements (RC circuit)

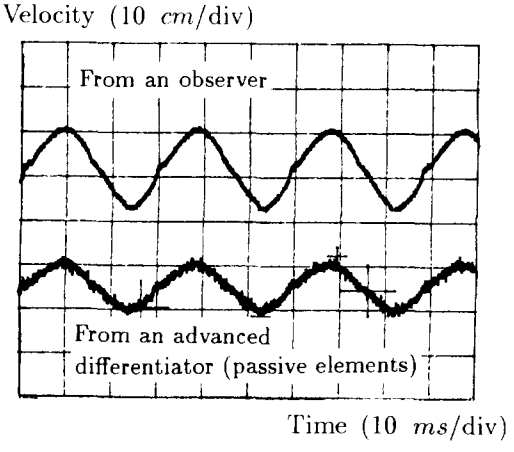

(b) active elements (RC circuit plus operational amplifiers)

Fig. 3 Comparison of the signals between observer and differentiator.

and the control input. From this state equation, an analog full-state observer is constructed. Details about the full-state observer are not treated here since it is well known theory. Advanced differentiators using passive elements (RC circuit) and active elements (RC circuit plus operational amplifiers) are shown in Fig. 3(a) and 3(b). They are ordinary differentiators with a high pass filter added to eliminate noise in the high frequency range. The velocity signal produced from the state observer is shown in the figure with that of an advanced differentiator. The differentiator produces severe noise compared to the observer.

If we can estimate the unknown disturbance and include that estimate in the controller law, the real disturbance of ω can be canceled, and the system behaves as if no disturbance is present. If we assume the disturbance is a constant or bias, it can be simply expressed as (Franklin, 1990) :

$$\dot{w}=0 \tag{6}$$

For disturbance estimation, we augment the system model described in Eqs. (4) and (5) with the disturbance model, so the augmented state equation becomes

$$\dot{x}_a=A_a x_a+B_a u, \tag{7}$$

where $x_a=[x_1, x_2, w]^T$. Then, the system matrices are

$$A_a=\begin{bmatrix}0 & 1 & 0\\ 0 & -\frac{c}{M} & \frac{1}{M}\\ 0 & 0 & 0\end{bmatrix},\quad B_a=\begin{bmatrix}0\\ \frac{K_a K_t}{m}\\ 0\end{bmatrix}$$

$$C_a=[1\ 0\ 0],\quad D_a=0.$$

The all control schemes discussed in the above is incorporated as shown in Fig. 4 $\hat{x}_1$ and $\hat{x}_2$ denote the observed position and velocity.

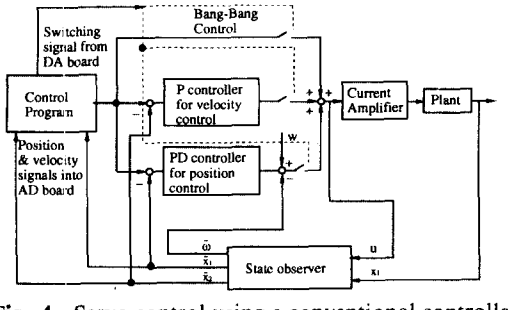

Fig. 4 Servo control using a conventional controller for the test of the tracking actuator.

3.3 Tracking servo system

The control objective of tracking actuator is simply to move the actuator from an initial state $\{x=x_i\ ;\ \dot{x},\ \cdots,\ \ddot{x},\ =0\}$ to a final state $\{x=x_f\ ;\ \dot{x},\ \ddot{x},\ \cdots,\ =0\}$ in a minimum time. The optimal control which achieves the minimum access time is always an extremal control and involves N-1 drive signal polarity reversals for a system with an Nth order state equation (Ananthanarayanan, 1982). The extremal control for the system described by Eqs. (4) and (5) has one polarity reversal from $+V_s$ to $-V_s$, at a switching point, x_s. If an input current u_1 is applied in $0\le x_1\le x_s$, the accelerating curve is obtained by solving the state equations, Eqs. (4) and (5). If an input current u_2 is applied in $x_s\le x_1\le x_f$, the decelerating curve is also obtained by solving the state equations, Eqs. (4) and (5). Figure 5 shows how the switching points are determined by graphical

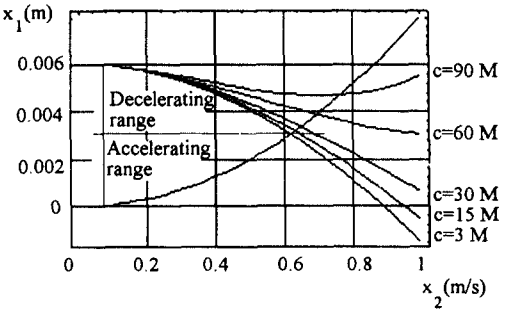

(a) when $u_1=u_2$

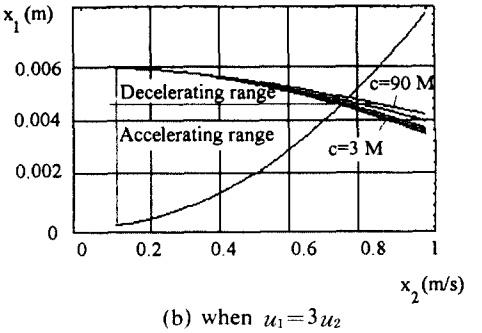

(b) when $u_1=3u_2$

Fig. 5 Variation of switching points for the different damping coefficients

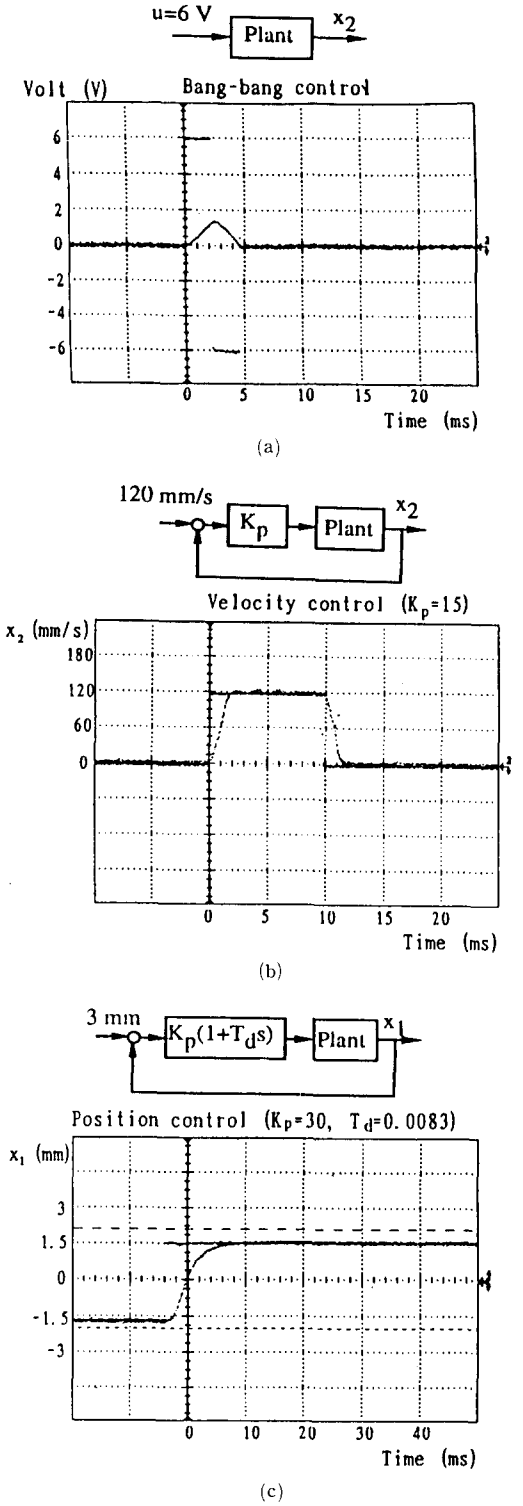

Fig. 6 Time responses for (a) bang-bang, (b) velo city, (c) position control.

representation in the phase plane (x_1-x_2). The switching point is determined by the intersection point of the two curves. When u_2 equals u_1, Fig. 5(a) shows how the switching points change for the different damping coefficients. If the damping coefficient, c is zero, the switching point occurs at the middle of the target point. As the damping coefficient increases, the switching point tends to shift upward to the target point. This implies that a slight change of the damping coefficient leads to the estimation of an incorrect switching point. But, when u_2 equals $3u_1$, the switching points occur at almost the same points even for the different damping coefficients as shown in Fig. 5(b). With the above consideration and power availability, we choose to use different control inputs as $u_1=5\,V$ and $u_2=7.5\ V$ respectively.

The separate responses for each control mode, i. e., bang-bang, velocity and position control, are shown in Fig. 6 with the controllers used. In the figure, K_p and T_d indicate the proportional gain and derivative time. u$=\pm 6\,V(200\ Hz)$ is applied for bang-bang control. 120 mm/s and 3 mm step inputs are applied for the velocity and position control, respectively with the corresponding gains. The settling time observed for each control mode are 5 ms, 2.5 ms, and 9ms.

The frequency response of tracking actuator is obtained in a low frequency region where the frequency characteristic of the coarse positioner is well represented. The bandwidth is defined as -3 dB magnitude ratio because the closed loop transfer function is considered as the 2nd order system. Figure 7 shows the frequency response of the position control. The bandwidth is around 100 Hz. The frequency response in a high frequency region shall be tested for the fine positioner.

The speed test with the hybrid control strategy is shown in Fig. 8 which shows control signals composed of the bang-bang input, velocity input, and position input and the corresponding velocity output profile. The input voltages of the accelerating range and decelerating range are chosen differently as 5 V and 7.5 V as discussed previously to reduce the variation of the switching point. We see that the average accessing time to

move 6 mm (average accessing distance of 3.5 inch disk) is around 23ms.

Figure 9 shows the accuracy test for the tracking actuator where the tracked position is represented in terms of the 12 bit A/D converter number. One bit represents 0.3 μm for this accuracy test. The tracking accuracy is much improved by using the disturbance observer as shown, and it is within ± 1 μm.

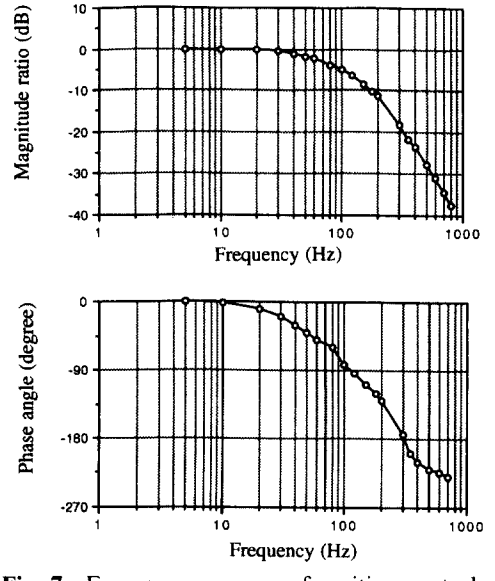

Fig. 7 Frequency response of position control.

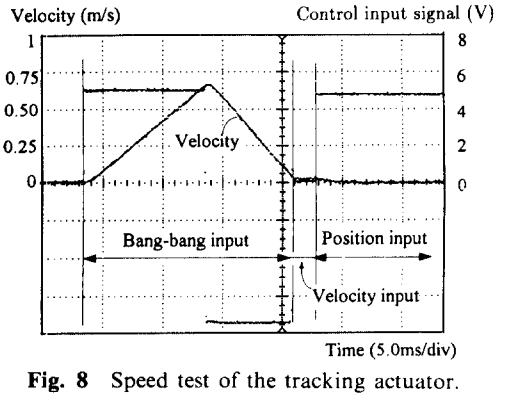

Fig. 8 Speed test of the tracking actuator.

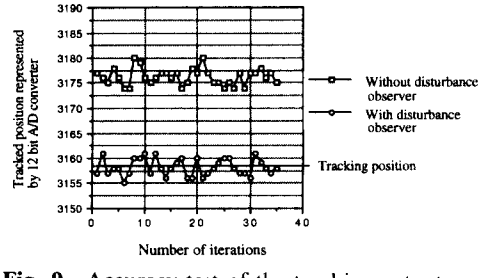

Fig. 9 Accuracy test of the tracking actuator.

4. Servo Control System Using an Advanced Controller

4.1 Why adaptive control?

Now, let's examine if we can improve the speed performance of the tracking actuator from control point of view. As the servo control for the tracking system presented this far, the bang-bang control plays the most important role of determining the tracking time. For best performance of bang-bang control, one needs to correctly calculate the switching point, where the maximum acceleration changes to the maximum deceleration. The switching point is calculated based on the system model. Since bang-bang control, however, is open-loop, its performance characteristics are dependent on the system components and the plant characteristics. This dependency makes it hard to determine the switching point accurately when the system model uncertainties exist. The inaccuracy of the switching point grows in a high frequency operating condition. i.e., high bang-bang input frequency. This fact indicates that we have a limitation in achieving fast tracking time using open-loop bang-bang control.

The approach taken to relieve this problem in this paper is to make the controlled plant follow, as closely as possible, a desired reference model whose switching point can be calculated easily and accurately. We build an adaptive loop to assure that the controlled plant always behaves as specified by means of a reference model that produces the desired output for a given input. This control method is called adaptive model-following control(AMFC). If the model reference is designed so that it has a high system bandwidth, tracking time can be reduced if we can assure that the error between the model reference and the real system approaches zero. Therefore, it can be said that the AMFC scheme is a good alternative for bang-bang control. Velocity and position control are switched in a row from the

AMFC scheme when it is finished.

Since we want to use the AMFC scheme instead of bang-bang control, our interest in the system modeling is to find out the relation between the input signal and actuator velocity. Therefore, the open loop transfer function of the velocity control system, G_m, is theoretically

$$G_m=\frac{v}{u}=\frac{K_aK_tK_v}{Ms+c}, \tag{8}$$

where K_v is the velocity sensor gain for the system tested. This theoretical model permits an easy calculation of the switching point, around at the middle of total tracking distance even in the high bang-bang input frequency. This fact, however, is really ideal, which is rarely seen in real systems because all physical plants tend to have system modeling errors.

The frequency response test for v versus u is experimentally performed to obtain real dynamic characteristics of the tracking system. The experimentally obtained amplitude ratio and phase angle are denoted by the legend 'o' in Fig. 10. The open loop transfer function of the real system can be most closely fitted to a second order system and denoted by the solid line:

$$G_p=\frac{114}{0.0005s^2+s+40}. \tag{9}$$

Now that we have obtained the real tracking system model, it remains to build an adaptive control loop to assure that the plant behaves as specified by means of a reference model that produces a desired output. Since the real dynamic system is characterized by a second-order transfer function, it seems natural to define the desired response by that of a reference model characterized also by a second-order transfer function,

$$G_r=\frac{114}{0.0001s^2+s+1}. \tag{10}$$

This transfer function assures that the system has a high bandwidth like the theoretical model because the coefficient of s^2 in Eq. (10) is small enough to be ignored.

4.2 AMFC design

If we take the velocity and acceleration as the state variables, the real plant to be controlled is described by

$$\dot{x}=A_px+B_pu_p, \tag{11}$$

where

$$x=\begin{bmatrix}x_1\\x_2\end{bmatrix}=\begin{bmatrix}v_a\\a\end{bmatrix}. \tag{12}$$

v_a and a are the tracking actuator velocity and acceleration, and u_p is the input voltage to the plant. Similarly, the reference model is described by

$$\dot{x}_m=A_mx_m+B_mu_m, \tag{13}$$

where

$$x_m=\begin{bmatrix}x_{m1}\\x_{m2}\end{bmatrix}=\begin{bmatrix}v_m\\a_m\end{bmatrix}. \tag{14}$$

v_m and a_m are the desired tracking actuator velocity and acceleration. u_m is the input voltage to the reference model. Here, (A_p, B_p), (A_m, B_m) are stablizable and, A_m is a Hurwitz matrix, i. e., the reference model is asymptotically stable.

We consider a parallel AMFC configuration with signal-synthesis adaptation as shown in Fig.

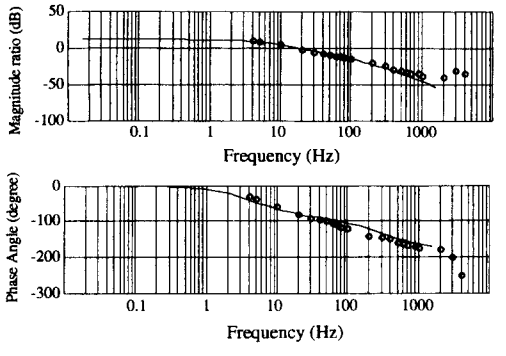

Fig. 10 Bode plot of theoretical model and experimentally obtained model.

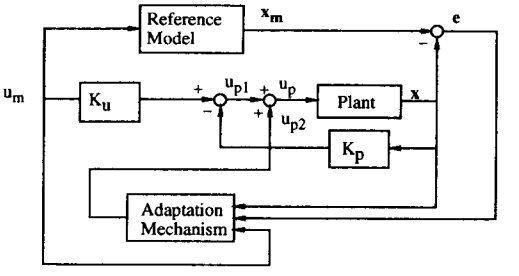

Fig. 11 A parallel AMFC configuration with signal-synthesis adaptation.

11. If we define

$$u_p = u_{p1} + u_{p2}, \tag{15}$$

where u_{p1} is the linear control signal, u_{p2} is the adaptation signal, we can then choose

$$u_{p1} = -K_p x + K_u u_m, \tag{16}$$

$$u_{p2} = \triangle K_p(e, t)x + \triangle K_u(e, t)u_m, \tag{17}$$

where K_p, K_u are linear control gains, and $\triangle K_p$ and $\triangle K_u$ are adaptation control gains having matrices of appropriate dimensions. The objective of the adaptation mechanism which will generate the two time-varying matrices $\triangle K_p(e, t)$ and $\triangle K_u(e, t)$ is to assure that the generalized state error, e, goes to zero under certain conditions.

Hyperstability and positivity theory say that the feedback system is asymptotically hyperstable if two conditions are satisfied (Landau, 1979) : the equivalent feed-forward block is a strictly positive real transfer function or matrix, and the feedback block must satisfy the Popov integral inequality. Let's first examine the adaptation mechanism in the feed-forward block. The feed-forward transfer function, $H(s)$, represented as

$$H(s) = (sI - A_m)^{-1} \tag{18}$$

should be a strictly positive real transfer matrix, or there must exist a P satisfying the Lyapunov equation such that

$$A_m^T P + P A_m = -Q, \tag{19}$$

in which Q is a positive definite matrix and the linear compensator D is

$$D = B_p^T P. \tag{20}$$

Next, for an adaptation mechanism in a feedback block, we introduce one of solutions of Popov integral inequality (Landau, 1979). The adaptation control gains, $\triangle K_p$ and $\triangle K_u$ are described using an integral plus proportional adaptation law as

$$\triangle K_p(e, t) = \int_0^t \phi_1(v, t, \tau)d\tau + \phi_2(v, t) + \triangle K_p(e, 0), \tag{21}$$

$$\triangle K_u(e, t) = \int_0^t \psi_1(v, t, \tau) + \Psi_2(v, t) + \triangle K_u(e, 0), \tag{22}$$

where

$$\phi_1(v, t, \tau) = F_a(t-\tau)v(\tau)[G_a(t)x(\tau)]^T, \quad \tau \geq t \tag{23}$$

$$\phi_2(v, t) = F'_a(t)v(t)[G'_a(t)x(t)]^T \tag{24}$$

$$\Psi_1(v, t, \tau) = F_b(t-\tau)v(\tau)[G_b(t)x(\tau)]^T, \quad \tau \geq t \tag{25}$$

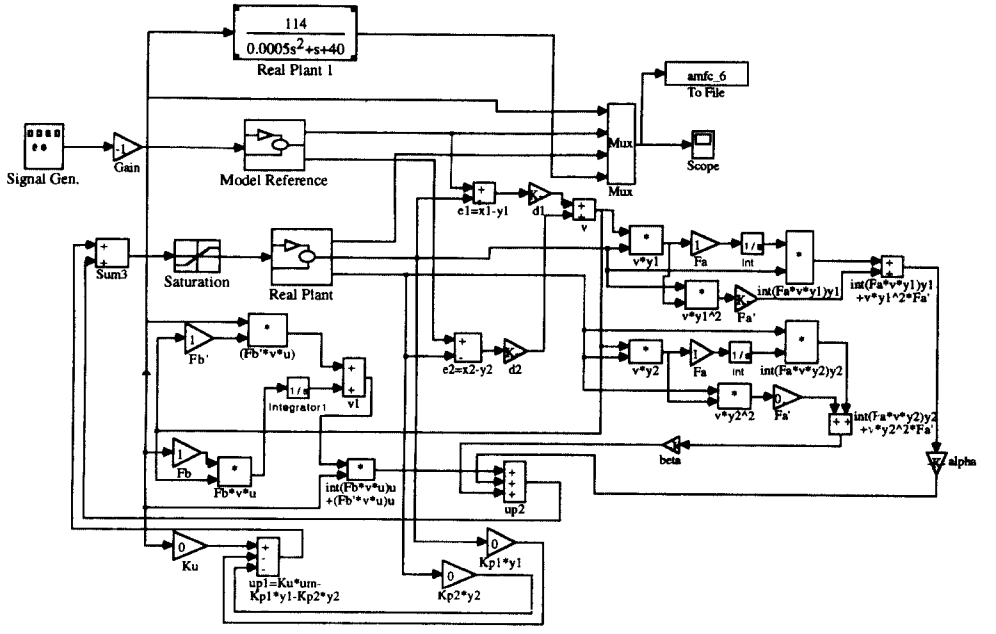

Fig. 12 Block diagram of AMFC control scheme.

$$\Psi_2(v,\ t)=F'_b(t)v(t)[G'_b(t)u(t)]^T, \quad (26)$$

where $F_a(t-\tau)$ and $F_b(t-\tau)$ are positive definite matrix kernels whose Laplace transforms are positive real transfer matrices with a pole at $s=0$. G_a and G_b are positive definite constant matrices; $F'_a(t)$, $F'_b(t)$, $G'_a(t)$ and $G'_b(t)$ are time-varying positive definite matrices for all $t\geq 0$.

Assuming that $\triangle K_p(e,0)=0$ and $\triangle K_u(e,0)=0$ we choose

$$F_a(t)=F_a>0,\ F'_a(t)=F'_a>0,$$
$$F_b(t)=F_b,\ F'_b(t)=F'_b,$$
$$G_a(t)=G'_a(t)=\begin{bmatrix}\alpha & 0\\ 0 & \beta\end{bmatrix},$$
$$\alpha>0,\ \beta\geq 0,\ G_b(t)=G'_b(t)=1. \quad (27)$$

Then, $\triangle K_p(e,\ t)$ and $\triangle K_u(e,\ t)$ are

$$\triangle K_p=\int_0^t F_a v x^T d\tau+F'_a v x^T$$
$$=[\alpha\int_0^t F_a v x_1 d\tau+\alpha F'_a v x_1,$$
$$\beta\int_0^t F_a v x_2 d\tau+\beta F'_a v x_2], \quad (28)$$

$$\triangle K_u=\int_0^t F_a v u d\tau+F'_b v u. \quad (29)$$

From Eqs. (16) and (17),

$$u_{p1}=-K_p x+K_u u_m=-K_{p1}x_1$$
$$-K_{p2}x_2+K_u u_m, \quad (30)$$

and

$$u_{p2}=\triangle K_p(e,\ t)x+\triangle K_u(e,\ t)u$$
$$=(\alpha\int_0^t F_a v x_1 d\tau)x_1+\alpha F'_a v x_1^2$$
$$+\beta(\int_0^t F_a v x_2 d\tau)x_2+\beta F'_a v x_2^2$$

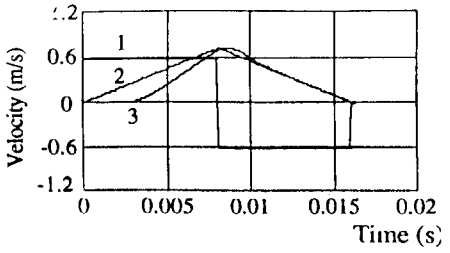

(a) $F_b=0.1$, $F'_b=0.1$, $d_1=70$, $d_2=0.014$

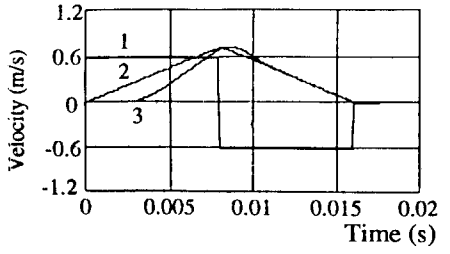

(b) $F_b=1$, $F'_b=0.1$, $d_1=70$, $d_2=0.014$

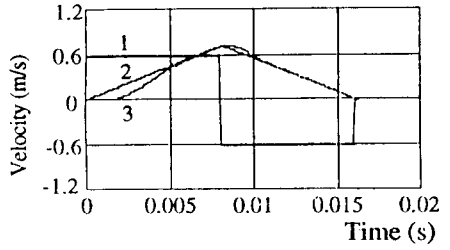

(c) $F_b=0.1$, $F'_b=1$, $d_1=70$, $d_2=0.014$

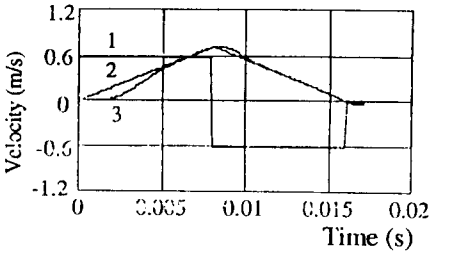

(d) $F_b=1$, $F'_b=1$, $d_1=70$, $d_2=0.014$

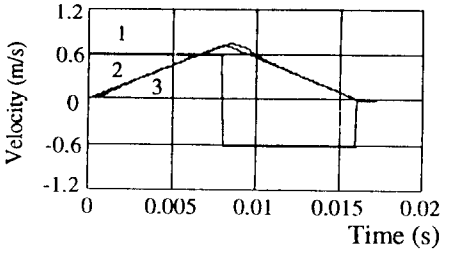

(e) $F_b=0.1$, $F'_b=0.1$, $d_1=700$, $d_2=0.077$

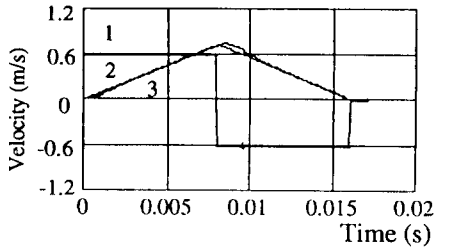

(f) $F_b=0.1$, $F'_b=0.1$, $d_1=70$, $d_2=0.077$

Fig. 13 Simulation result with respect to the different gains, F_b, F'_b, d_1, and d_2.

$$+\left(\int_0^t F_b v u d\tau\right) u + F'_b v u^2. \tag{31}$$

From Eq. (20)

$$v = De = d_1 e_1 + d_2 e_2. \tag{32}$$

The AMFC system designed above can be represented by the detailed configuration given in Fig. 12. All block diagrams are constructed in SIMULINK, which is a commercial system dynamics and control program that includes MATLAB (The MathWorks Inc., 1992).

To simulate real system environments as closely as possible, a maximum current constraint for the solenoid is imposed. The maximum and minimum currents are set to $+3$ A and -3 A, respectively. Since the sampling time currently used for servo control system of magneto-optical disk drive is less than 0.2 ms (Koumura, 1989), digital simulation uses 0.2 ms sampling time.

Several simulation results give a few design guidelines as a rule of thumb ; all linear control gains, K_u, K_{p1}, and K_{p2} have some freedom in its determination because they little influence on the tracking performance. Since β and F'_a are associated with the tracking acceleration they should keep small compared to α and F_a. α, β, K_u, K_{p1}, K_{p2}, F_a and F'_a are chosen as 1, 0.004, 1, 1, 1, 1, and 0.1 respectively.

Figure 13 shows how the tracking performance varies with respect to Q, F_b, and F'_b Two different Q matrices are chosen for comparison :

$$Q_1 = \begin{bmatrix} 10 & 0 \\ 0 & 0.001 \end{bmatrix} \text{ and } Q_2 = \begin{bmatrix} 100 & 0 \\ 0 & 0.001 \end{bmatrix}. \tag{33}$$

d_1 and d_2 corresponding to each Q matrix are obtained by solving the Lyapunov equation, Eqn (19). When $Q = Q_1$, we obtain $d_1 = 70$ and $d_2 = 0.014$ When $Q = Q_2$, we obtain $d_1 = 700$ and $d_2 = 0.077$. From Fig. 13(a), (b), (c) and (d), F'_b looks like a sensitive gain when $Q = Q_1$. However, F'_b does not influence much on the performance as shown in Fig. 13(e) and (f) when d_1 and d_2 have larger values as when $Q = Q_2$. Hence, we can conclude that Q is more sensitive than F_b and F'_b.

Figure 14 shows the experimental results of the

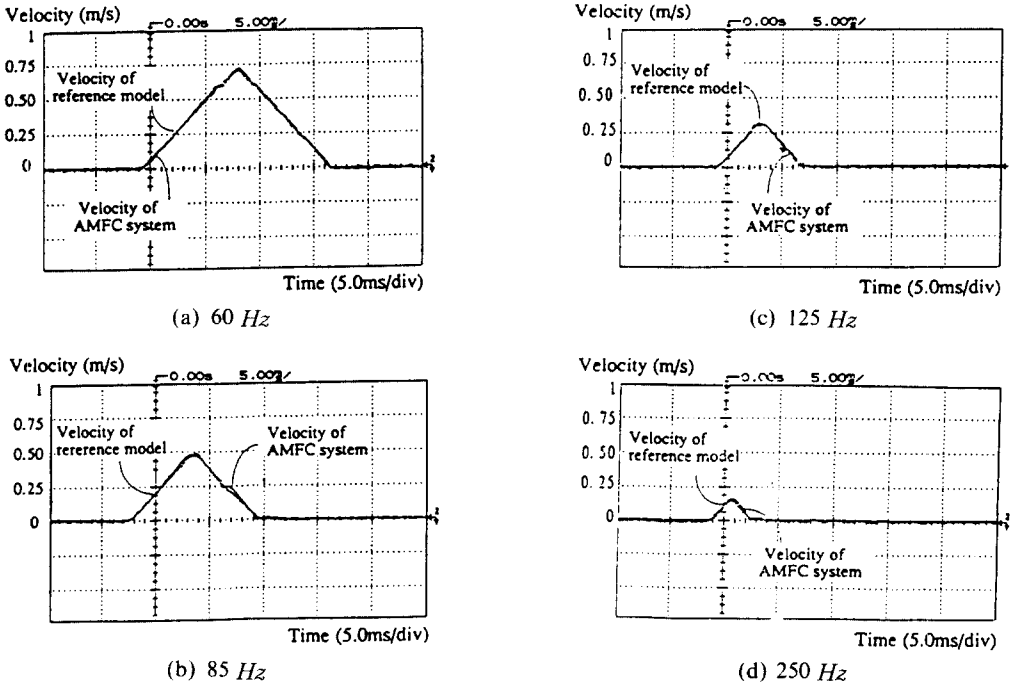

Fig. 14 The experimental results of the speed performance for different bang-bang input frequencies.

speed performance for different bang-bang input frequencies. The data acquisition and digital control module are built using a PC/C31 data acquisition board from Loughborough and an TMS320C31 digital signal processor. A IBM PC 486 serves as a host computer. The velocity responses from the real system, the reference model, and the AMFC system are shown together with the bang-bang input in the figures. The velocity using the AMFC system follows well the reference model up to 250 Hz. Therefore, we can conclude that the tracking time to move the average accessing distance of 3.5 inch disk, 6 mm, is around 17 ms from Fig. 14 (a) though we need to add a settling time which is determined in velocity and position control. If we assume the settling time is taken 1/6 of the tracking time (Hertrich, 1965), the average accessing time is about 20 ms.

This represents improvement over the 23 ms tracking time achieved by the hybrid control as shown in Fig. 8. It is also a marked improvement over the roughly 50 ms tracking times reported for commercial magneto-optical systems of comparable size.

5. Conclusion

To reduce the average accessing time of a magneto-optical (MO) disk drive, a newly developed tracking actuator has been designed. It would be used as a coarse positioner because most of accessing time is spent on coarse positioning.

The performance of the tracking actuator is tested with conventional control which is composed of a bang-bang control, velocity control, and position control. The condition of bang-bang input control is investigated to have the robustness for the system uncertainties and the disturbance observer is implemented with a state observer to increase the accuracy. 23 ms of accessing time and 1 μm of accuracy are achieved.

Then, adaptive model following control is applied to the system and its merit is demonstrated. Simulation and experimental results say that the average accessing time of 20 ms can be obtained by adopting this advanced control method. This is 3ms improvement over the 23 ms tracking time achieved by using the conventional control. It is a really remarkable improvement over the roughly 50 ms tracking time reported for commercial magneto-optical systems of comparable size.

As a future work, the tracking actuator will be applied to an magneto-optical disk instead of our artificially added sensor to make the magneto-optical disk be less sensitive to noise. This replacement can increase the tracking system bandwidth.

References

Ananthanarayanan, K.S., 1982, "Third-order theory and bang-bang control of voice coil actuator," *IEEE Trans. on Magnetics,* Vol. MAG-18, No. 3, May, pp. 888~892.

Franklin, Gene F., Powell, J. David, Workman, Michael L., 1990, *Digital Control of Dynamic Systems,* Addison-Wesley Publishing Company, California.

Hertrich, F. R., 1965, "Average Motion Times of Positioners in Random Access Devices," *IBM Journal,* Mar.

Koumura, K., Takizawa, F., Iwanaga, T., Inada, H., Yamanaka, Y., 1989, "High Speed Accessing using *Split,* Optical Head," *SPIE*, Vol. 1078, Data Storage Topical Meeting, pp. 239~243.

Landau, I. D. and Courtiol, B., 1974, "Design of Multivariable Adaptive Model Following Control Systems," *Automatica,* 10, pp. 483~494.

Park, Kyihwan, 1993. "Development of Tracking and Focusing Actuators for Magneto-Optical Disk Drive," Ph. D. Dissertation, Mechanical Engineering Department, University of Texas at Austin, August.

Park, Kyihwan, Busch-Vishniac, I., 1994. "A New Tracking System for Magneto-optical Disk Drives-Part I : Design," *KSME J.* Vol. 8, No. 3, pp. 255~263, 1994.

The MathWorks, Inc., 1992, User's Guide, SIMULINK Version 1.2, Natick, Ma 01760.